Article:
Wei, Y, Wang, C, Liu, X et al. (7 more authors) (2022) Co-encapsulation of curcumin and β-carotene in Pickering emulsions stabilized by complex nanoparticles: Effects of microfluidization and thermal treatment. Food Hydrocolloids, 122. 107064. ISSN 0268-005X

https://doi.org/10.1016/j.foodhyd.2021.107064

Co-encapsulation of curcumin and β-carotene in Pickering emulsions stabilized by complex nanoparticles: Effects of microfluidization and thermal treatment

Yang Wei[a,b,c], Chao Wang[a], Xin Liu[a], Alan Mackie[b], Mengke Zhang[c], Lei Dai [a], Jinfang Liu[a], Like Mao[a], Fang Yuan[a], Yanxiang Gao[a]*

[a]College of Food Science & Nutritional Engineering, China Agricultural University, Beijing, 100083, PR China
[b]Food Colloids and Processing Group, School of Food Science and Nutrition, University of Leeds, Leeds, LS2 9JT, UK
[c]School of Agriculture and Biology, Shanghai Jiao Tong University, 800 Dongchuan Road, Shanghai, 200240, PR China

Abstract
The objective of this study was to explore the influence of different particle concentrations (0.5%–3.0 %, w/v), microfluidization pressures (0–150 MPa) and heating temperatures (30–70 ◦C) on the physicochemical stability, microstructure, and in vitro digestion of β-carotene loaded Pickering emulsions stabilized by curcumin loaded complex nanoparticles. The optimum parameters for the fabrication of stable β-carotene loaded Pickering emulsions were 2.0 % (w/v) of particle concentration, 100 MPa of operating pressure and 60 ◦C of heating temperature. The co-encapsulation exhibited a synergistic effect on improving the photothermal stability of β-carotene and curcumin entrapped. During in vitro gastrointestinal digestion, the increased particle concentration (≥2.0 %, w/v) and heating temperature (≥50 ◦C) retarded the FFA release from the emulsions and reduced the bioaccessibility of curcumin and β-carotene through droplet flocculation. However, the lower pressure (≤100 MPa) promoted lipolysis and enhanced the bioaccessibility of nutraceuticals. The Pickering emulsion was designed for the co-delivery of curcumin and β-carotene via microfluidization and thermal treatment, which showed the great potential to be applied in the industrial production of functional foods and dietary supplements.

1. Introduction

There are numerous nutraceuticals that exert specific biological activities and curcumin and β-carotene are two representatives, which have been used in food industry (Sarkar & Mackie, 2020). Curcumin (Cur) is a natural polyphenol extracted from the turmeric (Sanidad, Sukamtoh, Xiao, McClements, & Zhang, 2019). Due to its various physiological functions, many studies focused on utilizing curcumin fortified into functional foods and dietary supplements (Chen, Wang, Feng, Jiang, & Miao, 2019; Dai, Wei, et al., 2018). However, the applications of curcumin-based products are limited because of its low solubility, poor bioavailability and vulnerability under various environmental conditions (light, heat, pH, and ionic strength) (Araiza-Calahorra, Akhtar, & Sarkar, 2018; Xiao, Nian, & Huang, 2015; Zou, Guo, Yin, Wang, & Yang, 2015). Among different carotenoids, β-carotene is one of the essential nutrients owing to its bioactivities (Weber & Grune, 2012). Plentiful researches have been conducted to incorporate β-carotene into foods (Mao, Wang, Liu, & Gao, 2018, March 24). Extensive delivery systems (e.g., nanoparticles, gels, emulsions) have been developed to improve the stability and bioavailability of β-carotene in food consumption (Wei, Sun, Dai, Zhan, & Gao, 2018; Wei, Tong, et al., 2020). Pickering emulsions (PEs) are extensively applied in chemical, cosmetic, pharmaceutical, and food industries. Most previous studies focused on their excellent stability against coalescence because of the steric barrier of particles at interfaces. Besides, PEs can be elaborately designed to deliver bioactives. Different nutrients have been encapsulated in nanoparticles at the liquid-liquid interface or dispersed into the oil phase (Liu & Tang, 2016; Tikekar, Pan, & Nitin, 2013; Winuprasith et al., 2018). In a previous study, we developed a Pickering emulsion-based vehicle for

the co-delivery of resveratrol and coenzyme Q10, which were loaded in different phases according to their solubilities (Wei, Yu, et al., 2020). The simultaneous use of nutraceuticals showed diverse advantages. The development of delivery systems co-loaded with multiple nutrients is limited by low loading capacity or immiscibility of nutrients. Although both of curcumin and β-carotene exhibit many biological activities, there has been no report available on the Pickering emulsion to encapsulate both of them. It is worth noting that curcumin and β-carotene exhibit distinct structures and polarities. Curcumin has a smaller molecular weight (368.13 Da) with many phenolic hydroxyl groups and β-carotene is a larger molecular com-pound (536.44 Da) with a long isoprenoid side chain (Donhowe & Kong, 2014; Weber & Grune, 2012). These structural differences generate different properties. β-Carotene (log P: 14.734) shows a greater hydrophobicity than curcumin (log P: 1.945) and it is hardly encapsulated into the interior of nanoparticles due to steric hindrance (Wei, Yang, Zhang, Dai, Tai, Liu, Mao, Yuan, et al., 2020; Zhang et al., 2019). Additionally, the bioaccessibility of curcumin and β-carotene can be enhanced in the Pickering emulsions with the formation of mixed micelles during lipolysis, facilitating their adsorption in the small intestine (Mulet-Cabero et al., 2020). The curcumin loaded nanoparticles can improve the interfacial antioxidant capacity of PEs to prevent β-carotene from degradation against light, heat and lipid oxidation (Fan, Liu, Gao, Zhang, & Yi, 2018; Wei, Yu, et al., 2020). Zein is a plant protein and more than 50 % of its protein composition is hydrophobic amino acids (Patel & Velikov, 2014). Due to its unique amphiphilic nature, zein can often self-assemble to form colloidal particles by adjusting the polarity of solvents (Wang & Padua, 2010). Propylene glycol alginate (PGA) is a characteristic amphiphilic polysaccharide, which could be integrated with zein to improve the hydrophilicity and stability of zein nanoparticles (Wei et al., 2018). Tea saponin (TS) is a natural small-molecule surfactant extracted from camellia seed (Zhu et al., 2019). According to a previous research, PGA and TS can be introduced into complex particles to improve the hydrophilicity of zein and control its microstructure, and improve the stability of nanoparticles (Wei, Li, et al., 2020). This study is aimed to explore the potential of using the zein-PGA-TS complex nanoparticle to encapsulate curcumin and stabilize β-carotene loaded Pickering emulsions.

Although a number of strategies have been developed to prepare emulsions (Håkansson & Rayner, 2018), the microfluidization is the most efficient way to produce smaller droplets with narrower size distributions (Bai & McClements, 2016; Håkansson et al., 2011; Mao, Yang, Xu, Yuan, & Gao, 2010; Perrier-Cornet, Marie, & Gervais, 2005). The droplet size of PEs usually reaches more than 10 μm, which is disadvantageous to the stability and macroscopic properties of food products. Nevertheless, only a few attempts were performed to prepare PEs using microfluidization. One recent study reported the use of a microfluidizer to produce cellulose nanocrystal (CNC)-stabilized PEs (Bai et al., 2019a). There has been no information on the influence of microfluidization parameters on physicochemical stability and structural features of PEs for the co-delivery of curcumin and β-carotene. When the oil fraction is fixed, the homogenization pressure and particle concentration are the two of most fundamental factors affecting the stability of PEs. The thermal treatment is considered as another important factor in the preparation of PEs using microfluidization, which can modulate the microstructure and stability of emulsions through affecting the particle properties and interparticle interactions. In a previous study, zein-PGA-TS complex nanoparticles were fabricated for delivery of curcumin, and subsequently the microstructure, molecular interactions and physicochemical stability of the nanoparticles have been comprehensively investigated (Wei et al., 2021). Based on the previous research, the curcumin loaded zein-PGA-TS complex nanoparticles were designed to stabilize β-carotene loaded Pickering emulsions. The effects of particle concentration, homogenizing pressure and heating temperature on the structure, stability, and in vitro digestion of Pickering emulsions were explored. Furthermore, new insights were provided into the modulation of lipid digestion and nutrient bioaccessibility of Pickering emulsions through microfluidization and thermal treatment. Our findings

proposed a new pathway for manufacturing nutraceutical Pickering emulsions to deliver curcumin and β-carotene simultaneously via microfluidization and thermal treatment.

2. Materials and methods

2.1. Materials

Zein (protein content: 91.3 %), lipase (pack size: L3126) and bile salts (pack size: 48305) were purchased from Sigma-Aldrich (USA), which reported that lipase activity is 100–500 units/mg protein (using olive oil). The bile salts are composed of 50 % deoxycholic acid sodium salt and 50 % cholic acid sodium salt. Propylene glycol alginate (PGA) (degree of esterification: 87.9 %) was kindly donated by Hanjun Sugar Industry Co. Ltd. (Shanghai, China). Curcumin (98 %) was purchased from China National Medicine Group Shanghai Corporation (Shanghai, China). Medium-chain triglycerides (MCT, Miglyol 812N) were purchased from Musim Mas (Medan, Indonesia). β-Carotene suspension (30 % by mass β-carotene in sunflower oil) was supplied by Xinchang Pharmaceutical Company, Ltd. (Xinchang, Zhejiang, China). Tea saponin (TS) was obtained from Han Qing Biological Technology Co. Ltd. (Hunan, China), which is a yellowish powder that contains around 51.8 % saponin. Absolute ethanol (99.99 %), solid sodium hydroxide and liquid hydrochloric acid (36 %, w/w) were obtained from Eshowbokoo Biological Technology Co., Ltd. (Beijing, China). All other chemical agents were of analytical grade.

2.2. Fabrication of curcumin loaded zein-PGA-TS complex nanoparticles

Briefly, 6.5 g zein, 1.50 g PGA, 0.50 g TS and 0.50 g curcumin were added into 1000 mL 70 % (v/v) aqueous ethanol solution in sequence with magnetic stirring at 600 rpm at 25 ◦C until their complete dissolution. Thereafter, the solutions were subjected to microfluidization at 100 MPa for 2 cycles by a Microfluidizer® processor model M-110EH (Microfluidics, Newton, MA, USA). All mixed solutions were then evaporated at 45 ◦C and the remaining volumes were set to 250 mL, which was then diluted with distilled water (pH 4.0) to 300 mL. The particle dispersions were centrifuged (Sigma 3k15, Germany) at 725×g for 10 min and the supernatants were collected. Part of samples was placed at 5 ◦C for further analysis and the others were lyophilized using a freeze-drying apparatus (Alpha 1-2D Plus, Marin Christ, Germany) to obtain powders for further characterization.

2.3.Preparation of β-carotene loaded Pickering emulsions stabilized by curcumin loaded complex nanoparticles

β-Carotene suspension (25 g, 30 wt% dispersed in sunflower seed oil) was first dissolved in MCT oil (225 g) at 140 ◦C for 30 s to form oil phase (1.5 wt% β-carotene in final emulsions). The primary emulsion was prepared by mixing 80 g of the nanoparticle dispersion with 80 g of oil phase at a speed of 18000 rpm using a blender (Ultra Turrax, model T25, IKA Labortechnic, Staufen, Germany). After the complete dispersion of oil phase, the dispersion was further homogenized for another 5 min to form the primary emulsion, and then it was subjected to the microfluidization. To ascertain the influence of particle concentration on the properties of PEs, all the primary emulsions were homogenized two times at 100 MPa. The PEs stabilized by different concentrations (0.50 %, 1.00 %, 1.50 %, 2.00 %, 2.50 % and 3.00 %, w/v) of the nanoparticles were termed as $PE_{0.50\%}$-HPM100, $PE_{1.00\%}$-HPM100, $PE_{1.50\%}$-HPM100, $PE_{2.00\%}$-HPM100, $PE_{2.50\%}$-HPM100 and $PE_{3.00\%}$-HPM100, respectively. Based on the preliminary experiments, different homogenization pressures (0, 50, 75, 100, 125 and 150 MPa) were imposed to prepare the PEs stabilized by 2.00 % (w/v) of the nanoparticles and the emulsions were named as $PE_{2.00\%}$-HPM0, $PE_{2.00\%}$-HPM50, $PE_{2.00\%}$-HPM75, $PE_{2.00\%}$-HPM100, $PE_{2.00\%}$-HPM125 and $PE_{2.00\%}$-HPM150, respectively. Besides, the effect of thermal treatment on primary emulsions was estimated by pre-heating the primary emulsions to 30, 40, 50, 60 and 70 ◦C, respectively. Thereafter, all emulsions were subjected to micro-fluidization at 100 MPa for 2 cycles immediately. The samples

were termed as $PE_{2.00\%}$-HPM100-30 ◦C, $PE_{2.00\%}$-HPM100-40 ◦C, $PE_{2.00\%}$- HPM100-50 ◦C, $PE_{2.00\%}$-HPM100-60 ◦C and $PE_{2.00\%}$-HPM100-70 ◦C, respectively.

2.4. Droplet size and surface charge

The droplet size and size distribution were measured after preparation of PEs for 12 h with a laser scattering size analyzer (LS230®, Beckman Coulter, USA). The samples were diluted with deionized water at 3000 rpm until an obscuration rate between 8 % and 12 % was obtained. The optical properties were applied as follows: a refractive index of 1.52 for MCT and absorption of 0.001, and a refractive index of 1.33 for the dispersant (deionized water) (Wei et al., 2019a). The volume-area ($D_{4,3}$) average diameters were calculated by following the equation below:

$$D4,3 = \frac{\sum nidi^4}{\sum nidi^3}$$

The n_i is the number of particles with a diameter of d_i.

The surface charge of oil droplets was determined by measuring the direction and velocity of droplet movement in an electric field using a Zetasizer NanoZS90 (Malvern Instruments, Worcestershire, UK). Emulsions were diluted to a final oil droplet concentration of 0.005 wt% with pH-adjusted deionized water (pH 4.0) to minimize multiple scattering effects. The data were collected from at least 10 sequential readings per sample after 120 s of equilibration and calculated using the Smoluchowski model. All measurements were performed in triplicate.

2.5. Quantitation of curcumin and β-carotene

The content of curcumin in complex nanoparticles was determined by following a previous reference with some modification (Dai, Wei, et al., 2018). Briefly, 2 mL of fresh emulsion was mixed with 8 mL of absolute ethanol through vortex oscillation for 2 min. Each of samples was centrifugated at 10000 g for 30 min, and the supernatant of sample after centrifugation was mixed with the same volume of hexane. Then the mixture was oscillated for 1 min and centrifugated at 725 g for 10 min. Thereafter, the supernatant (hexane, containing β-carotene) was removed and the remaining part was diluted to an appropriate con-centration (in the range of 0–6 μg/mL) with 80 % ethanol-water solution (v/v). Absorbance was measured with the aforementioned spectrophotometer at 426 nm. The concentration of curcumin was determined by referring to a standard curve. Entrapment efficiency (EE) of curcumin was calculated by following the equation below:

$$\mathrm{EE}\ (\%) = \frac{\text{encapsulated curcumin (mg)}}{\text{total curcumin input (mg)}} \times 100\%$$

The determination of β-carotene in emulsions was conducted ac-cording to a previous study (Wei, Tong, et al., 2020). All emulsions were diluted to an appropriate concentration, and then a mixed solvent (absolute ethanol/n-hexane=1:3) was used to extract the β-carotene entrapped in PEs. Absorbance was measured with a UV-1800 spectrophotometer (Shimadzu Corporation, Kyoto, Japan) at 450 nm. The content of β-carotene was analyzed using a standard curve of β-carotene prepared under the same condition. Entrapment efficiency (EE) was calculated by following the equation below:

$$\mathrm{EE}\ (\%) = \frac{\text{encapsulated } \beta-\text{carotene (mg)}}{\text{total } \beta-\text{carotene input (mg)}} \times 100\%$$

Encapsulated β-carotene or curcumin represents the mass of nutrients in PEs. Total β-carotene or curcumin input represents the total mass of nutrients added.

2.6. Physicochemical stability of Pickering emulsions

2.6.1. Physical stability

The physical stability of PEs was measured by the LUMiSizer (L.U.M. 290 GmbH, Germany) by accelerating the occurrence of instability phenomena such as coalescence and creaming (Wei et al., 2019a). The samples went through the centrifugal force, while near-infrared light illuminated the whole sample cell to assess the intensity of transmitted light as a function of time and position over the entire sample length simultaneously. The parameters used for the measurement were set as follows: 1.2 mL of emulsion; rotational speed, 3000 rpm; performed time, 3600 s; time interval, 20 s; temperature, 25 ◦C.

2.6.2. Photo stability

The photostability of curcumin and β-carotene in PEs against UV photolysis was tested. Briefly, 15 g of fresh sample was placed into transparent glass vial. Then samples were put into a controlled light cabinet (QSun, Q-Lab Corporation, Ohio, USA) for up to 4 h (Wei, Tong, et al., 2020). The retention rates of curcumin and β-carotene were plotted against individual treatment times. All experiments were per-formed in triplicate.

2.6.3. Thermal stability

The emulsions after 12 h storage at the ambient temperature (25 ◦C) were incubated in water bath (85 ◦C) for 60 min and then cooled down to 25 ◦C (Wei et al., 2020). After each treatment, the average droplet size and zeta-potential of PEs were measured after 12 h storage (25 ◦C) to acquire a stable state. Besides, the retention rates of curcumin and β-carotene entrapped in PEs were also detected after thermal treatment.

2.7. Confocal laser scanning microscopy

Confocal laser scanning microscopy (CLSM) (Zeiss780, Germany) was used to visualize the interfacial structure of droplets. The emulsions were stained with a mixed fluorescent dye solution consisting of Nile blue (0.1 %) and Nile red (0.1 %). The Nile blue was used to stain nanoparticles and the Nile red was applied to dye oil phase. Then the dyed emulsions were deposited on concave confocal microscope slides and gently covered with a cover slip (Dai, Sun, Wei, Mao, & Gao, 2018). The CLSM was operated using two laser excitation sources: an argon/krypton laser at 488 nm (Nile red) and a Helium Neon laser (He-Ne) at 633 nm (Nile blue).

2.8. Cryo-scanning electron microscopy

In the Cryo-SEM technique, the samples are vitrified with liquid nitrogen at a very low temperature, which can preserve the structure of emulsions in a frozen state and allow them to remain stable during the observation (Sriamornsak, Thirawong, Cheewatanakornkool, Burapapadh, & Sae-Ngow, 2008). The original structures of PEs were observed by Cryo-SEM. Then the images were captured using SEM (Helios NanoLab G3 UC, FEI, USA). The observation was performed at a working distance between 3 and 5 mm with TLD (Through Lens Detector) detection at 2 kV.

2.9. *In vitro* digestion, free fatty acid release and bioaccessibility

This study used an international standardized *in vitro* digestion model with some modifications (Minekus et al., 2014):

Gastric phase: 20 mL of the emulsion was mixed with 20 mL of simulated gastric fluid (SGF) containing 0.0032 g/mL pepsin to mimic gastric digestion. The pH was adjusted to 2.0 and the sample was then swirled at 150 rpm for 1 h at 37 ◦C. Small intestine phase: 20 mL of gastric digesta was transferred into a 100 mL glass beaker and then adjusted to pH 7.0. Thereafter, 20 mL of simulated intestinal fluid (SIF) containing 5 mg/mL bile salts, 0.4 mg/mL pancreatin and 3.2 mg/mL lipase was mixed with digesta in reaction vessel. The pH was adjusted to 7.0 and the samples were held under continuous vibration at 150 rpm for 2 h at 37 ◦C to mimic intestinal digestion. The degree of lipolysis was measured through the amount of free fatty acids (FFA) released. The amount of 0.25 M NaOH required to neutralize the released FFA through lipid digestion was determined by a pH-stat automatic titration unit (Metrohm, Switzerland, 916 Ti-Touch) (Xiao et al., 2018). The amount of FFA released was determined as the percentage of FFA (%) released during the digestion time (Li & Julian McClements, 2010):

$$FFA\ release\ rate\ (\%) = \frac{V_{NaOH} m_{NaOH} M_{lipid}}{2W_{lipid}} \times 100\%$$

where V_{NaOH} and m_{NaOH} represent the volume (L) and concentration (M) of NaOH solution needed to neutralize the FFA. W_{lipid} and M_{lipid} represent the initial mass (g) and molecular mass ($g \cdot mol^{-1}$) of the triacylglycerol oil.

The bioaccessibility of nutraceuticals was determined after intestinal digestion (Liu, Ma, Zhang, Gao, & Julian McClements, 2017). Part of the digesta was processed using a high-speed centrifuge at 15,000 rpm for 60 min at 4 ◦C. The micellar phase containing the solubilized nutraceutical was collected. The content of nutraceutical extracted from the initial emulsion and micelle fraction was determined according to the method described in 2.5. The bioaccessibility (%) was calculated by following the equation below:

$$Bioaccessibility\ (\%) = \frac{C_{micelle}}{C_{initial\ emulsion}} \times 100\%$$

where, $C_{micelle}$ and $C_{initial\ emulsion}$ are the contents of nutraceutical in the micelle fraction and the initial emulsion.

2.10. Statistical analysis

All the data obtained were average values of triplicate de-terminations and subjected to statistical analysis of variance using SPSS 18.0 for Windows (SPSS Inc., Chicago, USA). Statistical differences were determined by one-way analysis of variance (ANOVA) with Duncan's post hoc test and the least significant differences (p <0.05) were accepted among the treatments.

3. Results and discussion

3.1. Characteristics of curcumin loaded complex nanoparticles

The fundamental properties of curcumin loaded zein-PGA-TS complex nanoparticles were explored before the evaluation of Pickering emulsions, which served to understand the behaviour of particles at the interface. The complex nanoparticles showed a spherical shape with a uniform size (PdI: 0.109 ±0.015). The average size and zeta-potential of complex nanoparticles were 195.8 ±1.2 nm and -21.1 ±0.8 mV (Fig. S1A). The small size facilitated the adsorption of particles onto the interface with a higher desorption energy compared to traditional emulsifiers (Binks, Desforges, & Duff, 2007). The contact

angle ($\theta_{o/w}$) of complex nanoparticles was around 87.7 ±0.7◦ (Fig. S1B), exhibiting a more appropriate interfacial wettability than that of zein-PGA complex nanoparticles (76.6 ±1.2◦) (Wei, Tong, et al., 2020). The phenomenon interpreted that the addition of TS improved the strong hydrophilicity of complex nanoparticles, promoting the adsorption of nanoparticles at interfaces (French, Taylor, Fowler, & Clegg, 2015).

3.2. Droplet size and zeta-potential

As shown in Fig. 1A, the particle concentration showed a profound influence on the stability of PEs. At the lowest concentration (0.5 %, w/ v) of nanoparticles, the Pickering emulsion exhibited a relatively large droplet size (23.06 ±0.19 μm). The low concentration of nanoparticles was insufficient to cover all the surface of droplets. As the particle concentration was increased from 0.5 % to 1.5 % (w/v), the droplet size of PEs was reduced to 7.23 ±0.08 μm with the rise in zeta-potential from - 18.63 ±3.76 to - 28.30 ±0.41 mV. When the particle concentration was elevated from 1.5 % to 3.0 % (w/v), the droplet size of PEs was decreased slightly with a moderate reduction in its zeta-potential, which revealed that the sufficient adsorption of complex nanoparticles (over 2.0 %, w/v) strengthened the steric and electrostatic repulsion between droplets.

The influence of microfluidization pressure on droplet size and zeta- potential was investigated (Fig. 1B). The highest droplet size (10.42 ±0.04 μm) was observed in the emulsion without microfluidization. With the aid of microfluidization, the droplet size of PEs was decreased with the rise in pressure. As the pressure was increased from 50 to 150 MPa, the droplet size was reduced slightly from 6.75 ±0.05 to 6.27 ±0.02 μm. Meanwhile, the absolute zeta-potential value was elevated with the rise in pressure due to deflocculation and rupture of droplets, which could be attributed to the increased magnitude of the disruptive energy generated inside the microfluidizer (Bai et al., 2019a). Nevertheless, the droplet size was increased slightly when the pressure was raised from 100 to 150 MPa due to over-processing at the higher pressure (Bai et al., 2019b).

The influence of heating temperature on the droplet size of PEs via microfluidization was presented in Fig. 1C. At lower temperatures, the droplet size decreased from 6.19 ±0.02 to 5.81 ±0.03 μm when the temperature was elevated from 30 to 40 ◦C. This might be because the moderate rise of temperature could facilitate the disruption of large droplets into small ones through microfluidization and therefore retarding the droplet flocculation. When the temperature was over 40 ◦C, the droplet size was increased with the rise in temperature, along with the gradual decrease in zeta-potential. The rising temperature increased the probability of collision between droplets and promoted coalescence. Besides, the interfacial particles might aggregate at higher temperatures, causing the partial flocculation between droplets (Xiao, Li, & Huang, 2016). The growth of droplet size reduced the specific surface area of droplets where particles could be adsorbed. Meanwhile, the emulsion coalescence might cause the particles on the droplet sur-face to desorb, and decrease the negative charge provided by the particles at the interface.

The size distribution of different emulsions is presented in Fig. 1D. At the lowest particle concentration (0.5 %, w/v), the Pickering emulsion exhibited the largest droplet size with the most concentrated distribution. With the increase in particle concentration, the droplet size of Pickering emulsions was decreased with a more dispersed distribution. For instance, $PE_{1.00\%}$-HPM100 showed a bimodal distribution of droplet size with two peaks at 2 and 10 μm. The low particle concentration was insufficient to cover all the droplet surface and tended to form particle bridges between droplets. Without microfluidization, $PE_{2.00\%}$-HPM0 showed a bimodal distribution of droplet size with two peaks at 10 and 30 μm, which suggested that the partial coalesence between droplets occurred. In the presence of microfluidization, the droplets of Pickering emulsions were uniformly distributed in the range of 5–10 μm. Nevertheless, the introduction of thermal treatment did not affect the size distribution of Pickering emulsions.

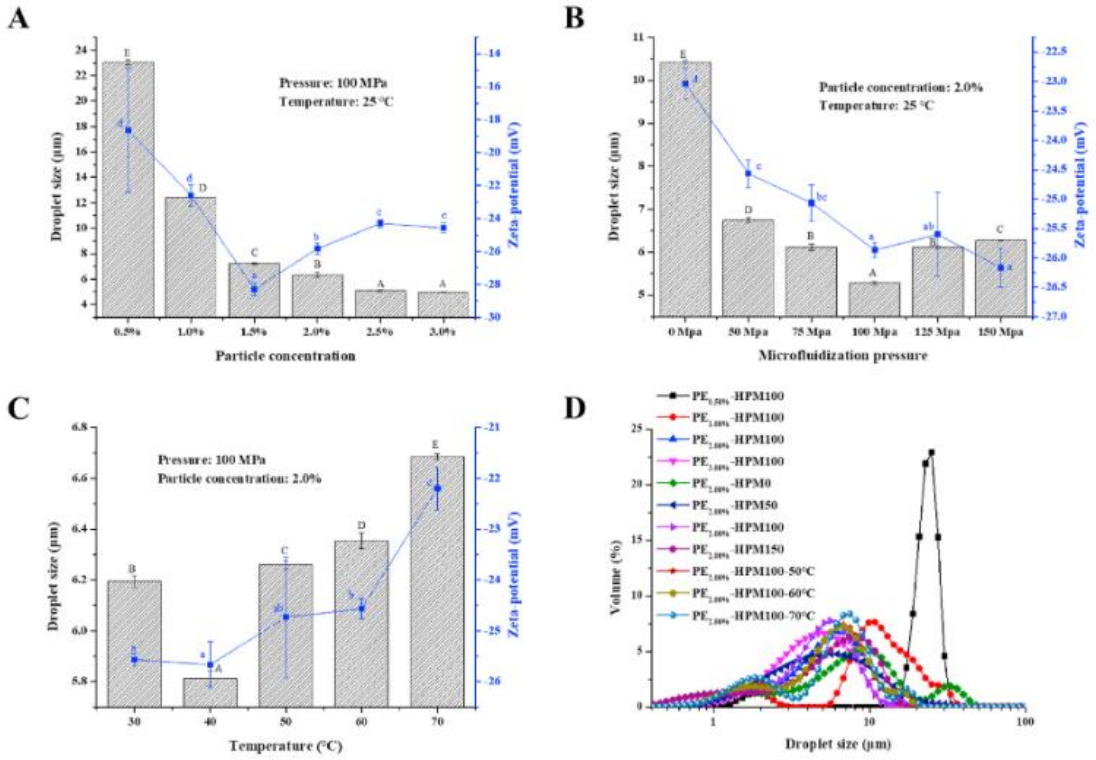

Fig. 1.Effects of particle concentration (A), microfluidization pressure (B) and heating temperature (C) on droplet size and zeta-potential of Pickering emulsions; droplet size distribution of Pickering emulsions (D). (Different superscript letters (A, B, C ...) in the figure indicate significant differences (p <0.05) in the droplet size of Pickering emulsions; different superscript letters (a, b, c ...) in the figure indicate significant differences (p <0.05) in the zeta-potential of Pickering emulsions).

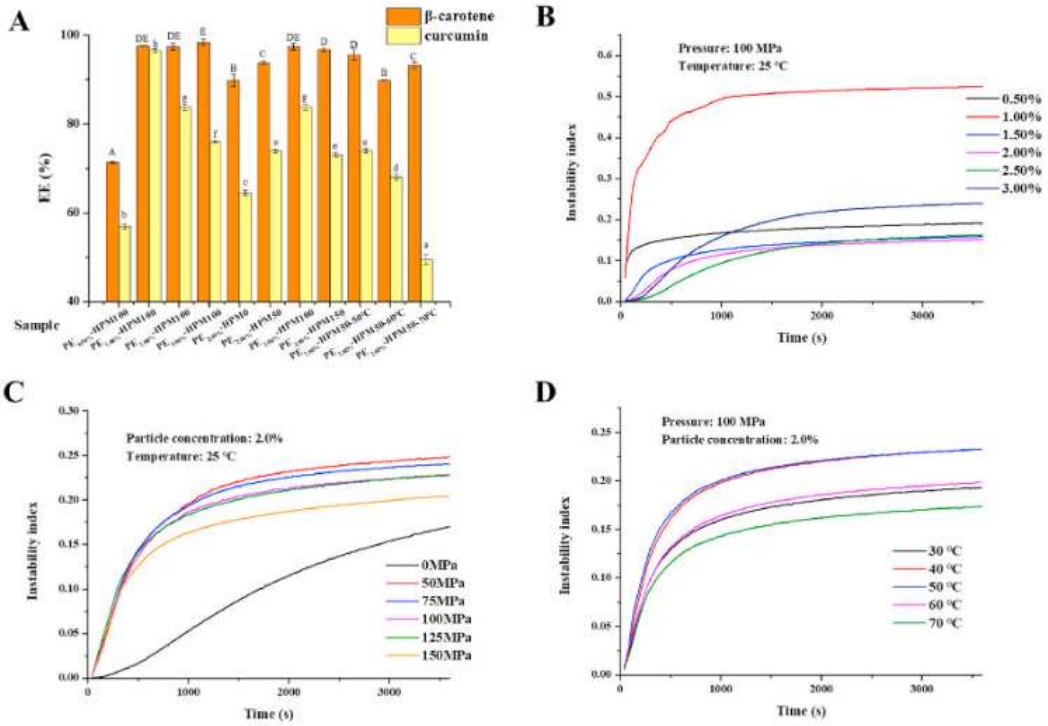

Fig. 2.Encapsulation efficiency (EE) of β-carotene and curcumin in Pickering emulsions (A); impacts of particle concentration (B), microfluidization pressure (C) and heating temperature (D) on physical stability of Pickering emulsions. (Different superscript letters (A, B, C ...) in the figure indicate significant differences (p <0.05) in EE of β-carotene; different superscript letters (a, b, c ...) in the figure indicate significant differences (p <0.05) in EE of curcumin).

3.3. Encapsulation efficiency of curcumin and β-carotene

To ascertain the encapsulation efficiency (EE) of nutraceuticals, the EE values of curcumin and β-carotene in the freshly prepared emulsions were determined. Among all the samples, the lowest EE of β-carotene was observed in $PE_{0.50\%}$-HPM100 due to the lowest particle concentration (Fig. 2A). The low concentration of particles was insufficient to cover the droplet surface and stabilize emulsions with their large droplet size, thus further causing the more loss of bioactives during the emulsion preparation. The low concentration of particles caused more exposure of droplet surfaces to the external environment, resulting in chemical degradation of β-carotene due to light, heat, oxygen and other external stresses. When the particle concentration was elevated to 1.0 % (w/v), the EE values of β-carotene and curcumin in $PE_{1.00\%}$-HPM100 increased to 97.58 ±0.12 % and 96.49 ±0.46 %, respectively. The result demonstrated that the increased concentration of nanoparticles could stabilize PEs with the smaller droplet size. With the rise in the particle concentration, the EE of β-carotene remained constant, but the EE of curcumin was decreased correspondingly. This phenomenon interpreted that the droplet surface has been saturated by complex nanoparticles, and therefore the excessive nanoparticles no longer adsorbed onto the interface and precipitated.

Without microfluidization, the EE of β-carotene and curcumin in $PE_{2.00\%}$-HPM0 were 89.86 ±1.33 % and 64.51 ±0.60 %, respectively. With the increase in the pressure from 0 to 100 MPa, the EE of β-carotene and curcumin were elevated to 97.39 ±0.76 % and 83.76 ±0.68 %, respectively, which were consistent with their smaller droplet sizes. The enlarged specific surface area allowed more nanoparticles to occupy the interface, thereby enhancing the EE of curcumin (Binks, 2002; Dickinson, 2017). Nevertheless, as the pressure was further elevated to 150 MPa, the EE of curcumin was slightly reduced with the constant EE of β-carotene, which was similar to the increased droplet size. Besides, the higher pressure might induce the slight growth of operating temperature inside the microfluidizer, thus resulting in a loss of curcumin due to thermal degradation (Bai et al., 2019c; Wei et al., 2021).

The influence of heating temperature before microfluidization on the EE of nutraceuticals is presented in Fig. 2A. When the temperature was elevated from 50 to 70 ◦C, the EE of curcumin entrapped was decreased from 73.98 ±0.48 % to 49.45 ±1.08 % with the fixed particle concentration and pressure. Curcumin was sensitive to heat and prone to degrade at higher temperatures (Bordoloi & Kunnumakkara, 2018). Although the nanoparticles provided a better protection for curcumin against heat compared to its free state, there was still a loss of curcumin at a higher temperature (Dai, Wei, et al., 2018). Nevertheless, the EE of β-carotene remained stable after thermal processing at higher temperatures. The β-carotene entrapped in oil phase became much more stable than the curcumin loaded in nanoparticles, indicating that the interfacial nanoparticles effectively inhibited chemical degradation of β-carotene with enhanced thermal stability (Yi, Liu, Zhang, & Gao, 2018). The phenomenon indicated that the interfacial composition (especially particle level) was vital to the feasibility of the Pickering emulsion as an effective carrier of nutraceuticals (Wei, Yu, Lin, Yang, Tai, Liu, Mao, Yuan, et al., 2020b).

3.4. Physicochemical stability of Pickering emulsions

3.4.1. Physical stability

Fig. 2B showed the influence of particle concentration on the physical stability of PEs. At the lowest particle concentration (0.5 %, w/v), the emulsion exhibited a stable state with the largest droplet size. The insufficient nanoparticles were incapable of covering all droplet surface, and therefore the Pickering emulsion exhibited an obvious aggregated state. As the surface density was below the saturation coverage, adjacent droplets joined together to form a stable non-spherical droplet through particle bridging known as arrested coalescence (Pawar, Caggioni, Ergun, Hartel, & Spicer, 2011). The aggregated droplets could be stabilized through sharing a single bridging layer of particles instead of

total coalescence, which provided a good stability at the low concentration of particles (Dickinson, 2017). When the particle concentration was 1.0 % (w/v), the stability of Pickering emulsion was reduced compared to other samples. The phenomenon might be attributed to particle bridging at interfaces, which induced the coalescence between droplets. With further an increase in particle concentration from 1.5 % to 2.5 % (w/v), the physical stability of PEs was improved, and the closely packed particles saturated the droplet surface strengthening steric and electrostatic repulsion. When the particle concentration reached 3.0 % (w/v), a slight decrease in the emulsion stability was observed, unraveling that excessive particles in the continuous phase induced the slight aggregation due to the enhanced osmotic pressure through the depletion flocculation.

Surprisingly, the Pickering emulsion without microfluidization showed a better physical stability than other samples (Fig. 2C). The droplet size was decreased gradually with the rise of applied pressure. On one hand, the larger size facilitated the closely approaching droplets in the emulsions with an obvious aggregation state. On the other hand, the droplets with larger size reduced the surface area exposed, facilitating the formation of a densely packed particle layer. Unlike the surfactant-covered emulsions, the nanoparticles almost irreversibly adsorbed on the interface with an intermediate wettability, which provided sufficient steric and electrostatic effect against coalescence (Dickinson, 2017). In spite of showing a larger droplet size through simple high-speed shearing, the Pickering emulsion demonstrated a long-term stability with a densely packed particle layer. As the pressure was elevated from 50 to 150 MPa, the physical stability was slightly improved with decreased droplet size.

Moreover, the stability of PEs was dependent on the heating temperature before microfluidization (Fig. 2D). As the temperature was elevated from 30 to 40 ◦C, the emulsion stability was visibly reduced due to the smaller droplet size and more bridges formed between droplets. As the temperature was further increased from 50 to 70 ◦C, the physical stability was enhanced with the increased droplet size. Generally, larger droplets in traditional surfactant-stabilized emulsions were under higher risk of further aggregation and coalescence. Nevertheless, the PEs suppressed the risk and exhibited the excellent physical stability with the densely packed particle-laden interface (McClements & Gumus, 2016; Wei, Tong, Dai, Ma, Zhang, Liu, Mao, Yuan, et al., 2020).

3.4.2. Photo stability

Among all samples, β-carotene was degraded most quickly in PE1$_{.00\%}$-HPM100 (Fig. 3A). After 4 h of light exposure, the retention rate of β-carotene was decreased to 46.36 ±2.08 % in PE$_{1.00\%}$-HPM100 compared to 80.83 ±1.34 % in PE$_{3.00\%}$-HPM100. Besides, the retention rate of β-carotene in PEs was consistent with their physical stability. With increasing the particle concentration, the chemical stability of β-carotene was reduced from PE$_{0.50\%}$-HPM100 to PE$_{1.00\%}$-HPM100, and reversely improved from PE$_{1.00\%}$-HPM100 to PE$_{3.00\%}$-HPM100, indicating that the physical stability was associated with chemical degradation of β-carotene at lower particle concentrations. When the particle concentration reached full saturation coverage, the retention rate of β-carotene was enhanced with the rise in particle level. A closely packed curcumin-loaded particle layer imparted an antioxidant ability to the interface, which provided a better protection for β-carotene against UV radiation (Xiao et al., 2016).

Comparably, the applied pressure showed a less effect on the photo stability of β-carotene in PEs. The retention rate of β-carotene in PE2.00%- HPM0 was 79.01 ±0.78 %. With the aid of microfluidization, there was a slight increase in the chemical stability of β-carotene. Interestingly, the heating temperature exhibited a more complex influence on the chemical stability of β-carotene in PEs against light. As the temperature was increased from 50 to 60 ◦C, the retention rate of β-carotene was elevated from 75.40 ±0.74 % to 88.03 ±1.15 % after 4 h of light exposure. Through the observation of cryo-SEM, the thermal treatment facilitated the formation of bridges between the nanoparticles at the interface (Fig. 6). The phenomenon implied that the network connected by particle bridges might protect β-carotene in lipid droplets through reducing the transmit of UV light as a physical barrier (Liu,

Wang, Xu, Sun, & Gao, 2016). When the temperature was elevated to 70 ◦C, the retention rate of β-carotene was decreased to 80.44 ±1.43 % in A4-HPM100-70 ◦C, which verified that the higher temperature disrupted the particle bridges in the Pickering emulsion, thus leading to a declination in the stability of β-carotene against UV radiation (Wei, Tong, et al., 2020).

Compared with β-carotene, the curcumin loaded in complex nanoparticles at the interface was less stable under light (Fig. 3B). With the continuous rise in particle concentration, the retention rate of curcumin was decreased and reached the minimum (46.36 ±2.08 %) in $PE_{1.00\%}$- HPM100 after 4h of exposure to light, which was similar to the chemical stability of β-carotene. Thereafter, the retention rate of curcumin was increased as the particle concentration was increased from 1.00 % to 3.00 % (w/v). The densely packed particle layer not only endowed the Pickering emulsion with the excellent long-term stability through steric and electrostatic repulsion, but also protected the interfacial layer loaded with nutraceuticals (Wei, Yu et al., 2020a). When the excessive particles existed, the interfacial structure might be transformed into a multilayer arrangement, with one or more extra layers of ordered monodisperse hard spheres accommodated in the inter-droplet region (Dickinson, 2015), which provided an associated kinetic structural barrier that conferred further steric protection to limit the transmit of light (Dickinson, 2017; Wei, Tong, et al., 2020). Similarly, the chemical stability of curcumin was slightly improved with the rise in the pressure. As the heating temperature was increased from 50 to 60 ◦C, the retention rate of curcumin in PEs was enhanced from 60.29 ±1.73 % to 79.13 ±0.87 %. Nevertheless, when the temperature reached 70 ◦C, the retention rate of curcumin was reduced to 68.57 ±2.01 %. The thermal treatment promoted the formation of particle bridges and protected the curcumin loaded in nanoparticles through reducing the penetration of light. The similar phenomenon was reported in other recent studies (Dai, Wei, et al., 2018; Wei, Yu, et al., 2019). It was noted that the higher temperature could break the particle bridges in PEs, thus damaging the photo stability of curcumin.

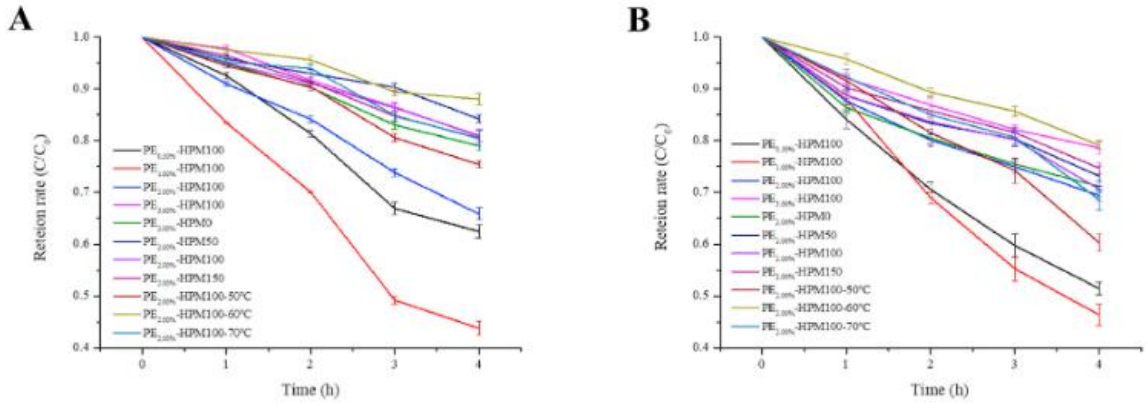

Fig. 3. Photo stability of curcumin (A) and β-carotene (B) encapsulated in Pickering emulsions.

3.4.3. Thermal stability

The droplet sizes of $PE_{0.50\%}$-HPM100 and $PE_{1.00\%}$-HPM100 were increased greatly after thermal processing (Fig. 4A). At a higher particle concentration, the droplet size of PEs remained more stable. While the concentration of particles was far below saturated coverage, a severe coalescence among droplets might occur during thermal treatment (Pawar et al., 2011). On the contrary, the presence of a closely packed layer of particles could improve the thermal stability of PEs and prevent the total coalescence. An obvious increase occurred in the droplet size of $PE_{2.00\%}$-HPM0 after thermal treatment. Heating showed a greater effect on PEs with a larger particle size, causing the flocculation of droplets. After the microfluidization, the droplet size of PEs at rational pressures ($PE_{2.00\%}$-HPM50 and $PE_{2.00\%}$-

HPM100) still kept stable, which improved the thermal stability of the emulsions through reducing the droplet size. Nevertheless, the droplet size of $PE_{2.00\%}$-HPM150 was increased, indicating that the higher pressure might disrupt the steric hindrance between droplets. In terms of the influence of heating temperature on the stability of PEs, there was a slight increase in the droplet size of $PE_{2.00\%}$-HPM100-50 ◦C. With the increase in heating temperature, there was a more obvious increase in the droplet size of PEs at 60 and 70 ◦C. Comparably, the effect of heating temperature on the thermal stability of PEs was much less than those of the particle concentration and operating pressure.

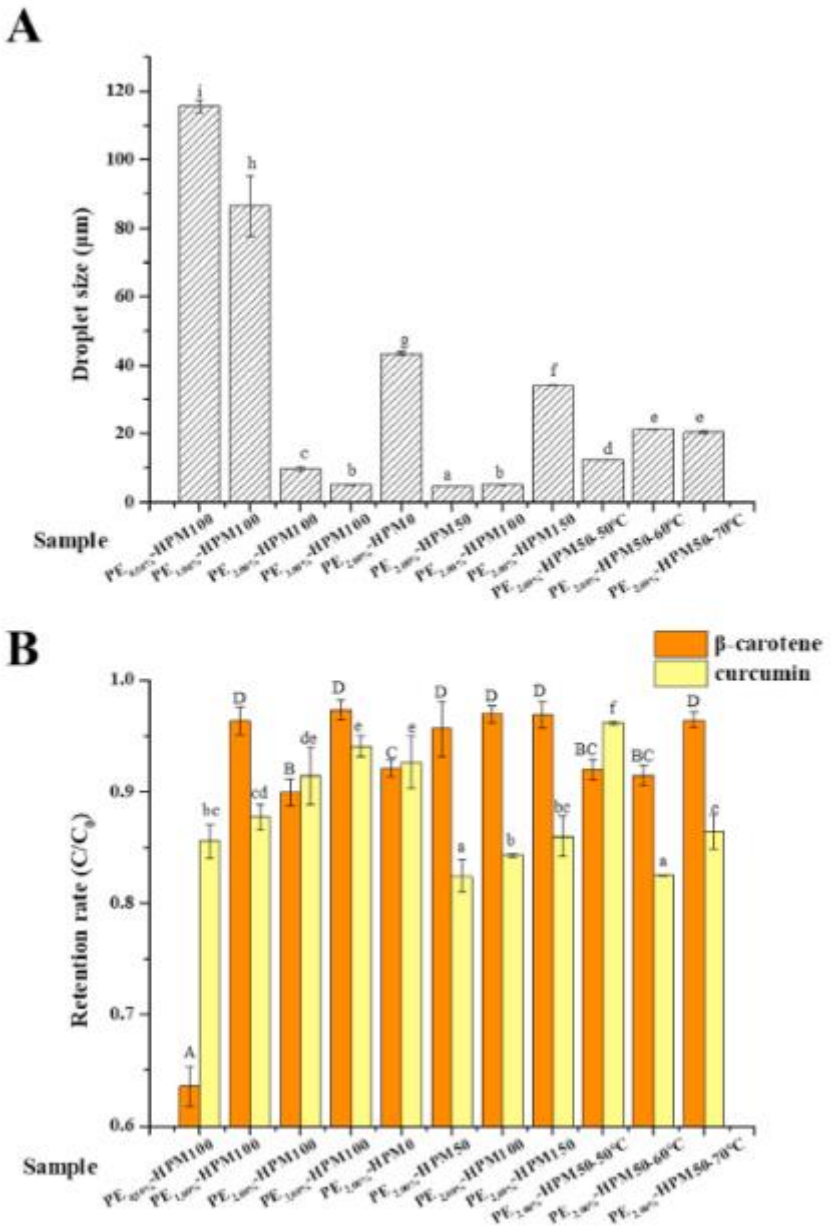

Fig. 4.Influence of thermal treatment on droplet size (A) of Pickering emulsions and chemical stability of β-carotene and curcumin (B) entrapped in Pickering emulsions. (Different superscript letters (A, B, C ...) in the figure indicate significant differences (p <0.05) in retention rate of β-carotene; different superscript letters (a, b, c ...) in the figure indicate significant differences (p <0.05) in retention rate of curcumin).

Among all samples, the lowest retention rate of β-carotene was observed in $PE_{0.50\%}$-HPM100, interpreting that a low concentration of nanoparticles was insufficient to protect β-carotene against

thermal degradation (Fig. 4B). With the increase in particle concentration, the thermal stability of β-carotene was improved due to enhanced interfacial antioxidant activity and steric repulsion (Liu et al., 2016; Wei, Yu, et al., 2020). The thermal stability of curcumin was enhanced with the increase in particle concentration, revealing that the curcumin loaded in nanoparticles and β-carotene encapsulated in droplets could protect each other against heat with a synergistic effect.

The retention rate of β-carotene in PEs was continuously increased with the rise in the operating pressure, which meant better thermal stability of β-carotene in the emulsions with smaller droplet sizes. At 50 MPa, the retention rate of curcumin loaded in nanoparticles was significantly (p <0.05) decreased from 92.64 ±2.33 % to 82.42 ±1.48 %. There was a slight increase in the retention rate of curcumin as the operating pressure was elevated from 50 to 150 MPa. The phenomenon demonstrated that the smaller droplet size was beneficial to protect the β-carotene encapsulated, but detrimental to the thermal stability of the curcumin loaded in nanoparticles. In terms of thermal treatment, the effect of heating temperature on the thermal stability of curcumin was greater than that of β-carotene. With the temperature increasing, the retention rate of curcumin was decreased and the retention rate of β-carotene was increased. The finding revealed that the curcumin loaded in nanoparticles at interfaces protected the β-carotene entrapped in droplets, and the rigid and anti-oxidant interfacial layer improved the thermal stability of β-carotene. Nevertheless, compared to PE2.00%-HPM100, the thermal stability of nutraceuticals entrapped in PEs was not improved with the combined microfluidization and heating.

3.5. Microstructure

Confocal fluorescence microscopy was utilized to analyze the interfacial structure by labelling nanoparticles and oil phase. All emulsion droplets showed regular spheres with a shell of particles (Fig. 5). The particle concentration exhibited a remarkable impact on the morphology of droplets. As the particle concentration increased, the droplet size decreased gradually even at higher concentrations, some particles were present in the continuous phase. In the absence of microfluidization, the droplets were stacked closely together, nevertheless, no coalescence was observed in the presence of particle-laden interface. With the pressure increasing from 0 to 100 MPa, there was a gradual declination in the droplet size. As the pressure was further elevated above 100 MPa, the droplet size remained constant with a more uniform distribution. The higher pressure promoted the disaggregation between droplets and retarded the droplet flocculation. Thermal treatment showed no significant impact on the microstructure of Pickering emulsions, although some droplets with larger sizes were observed at 30 and 50 ◦C due to the partial coalescence induced by heating.

As observed by cryo-SEM, the dense particles were attached at the interfaces (Fig. 6). As the particle concentration increased, the distribution density of particles attached at the interface was elevated. A spatial network structure occurred between droplets with the increase in particle concentration. At the highest particle level (3.0 %, w/v), the network of particles was substantially generated and the particle bridges were formed between droplets, dependent on the concentration and wettability of particles. The hydrophilicity promoted the particles entering into the continuous phase and facilitated the bridge formation (French et al., 2015; Wei, Tong, et al., 2020). The influence of applied pressure on the interfacial structure of PEs was also investigated. Without microfluidization, a number of bridged particle structures were observed on the droplet surface. However, after microfluidization treatment, only densely packed particles were found on the surface of droplets without bridging. When the pressure was elevated further to 150 MPa, the droplet surface became more wrinkled and the particle density was visibly reduced. The higher pressure might facilitate the partial desorption of interfacial particles. Additionally, the bridging between particles gradually disappeared with the pressure rising, which unravelled that microfluidization could break the bridging flocculation between

particles. Meanwhile, the decreased droplet size exposed more interfacial area, hence the particle distribution became more loose at the interface (French et al., 2015).

With the temperature rising, the droplet size of PEs was increased continuously (Fig. 6). When the temperature was elevated from 40 to 60 ◦C, the thermal treatment accelerated the motion of droplets and increased the probability of collision between droplets, which was more prone to bridging formation (Wei et al., 2019b). Nevertheless, as the temperature was elevated to 70 ◦C, there existed less bridges between droplets in the Pickering emulsions. The emulsion flocculation indicated that the higher temperature was capable of pulling two bridged droplets apart, and coalescence dominated over bridging (Pawar et al., 2011). Since the collisions of droplets led to particle bridging, and the extent of droplet flocculation increased when the temperature was increased continuously (French et al., 2015).

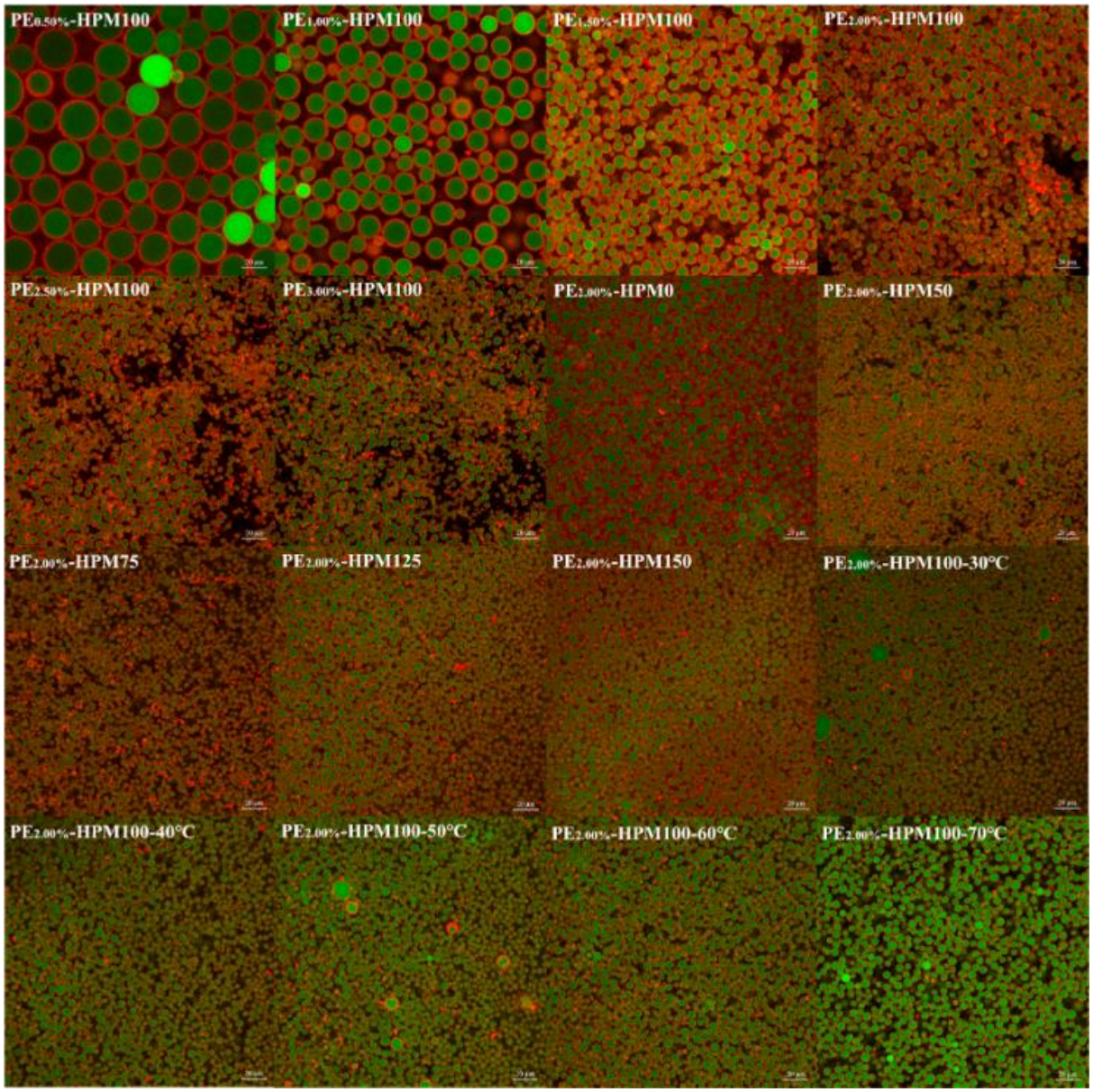

Fig. 5.CLSM images of different Pickering emulsions.

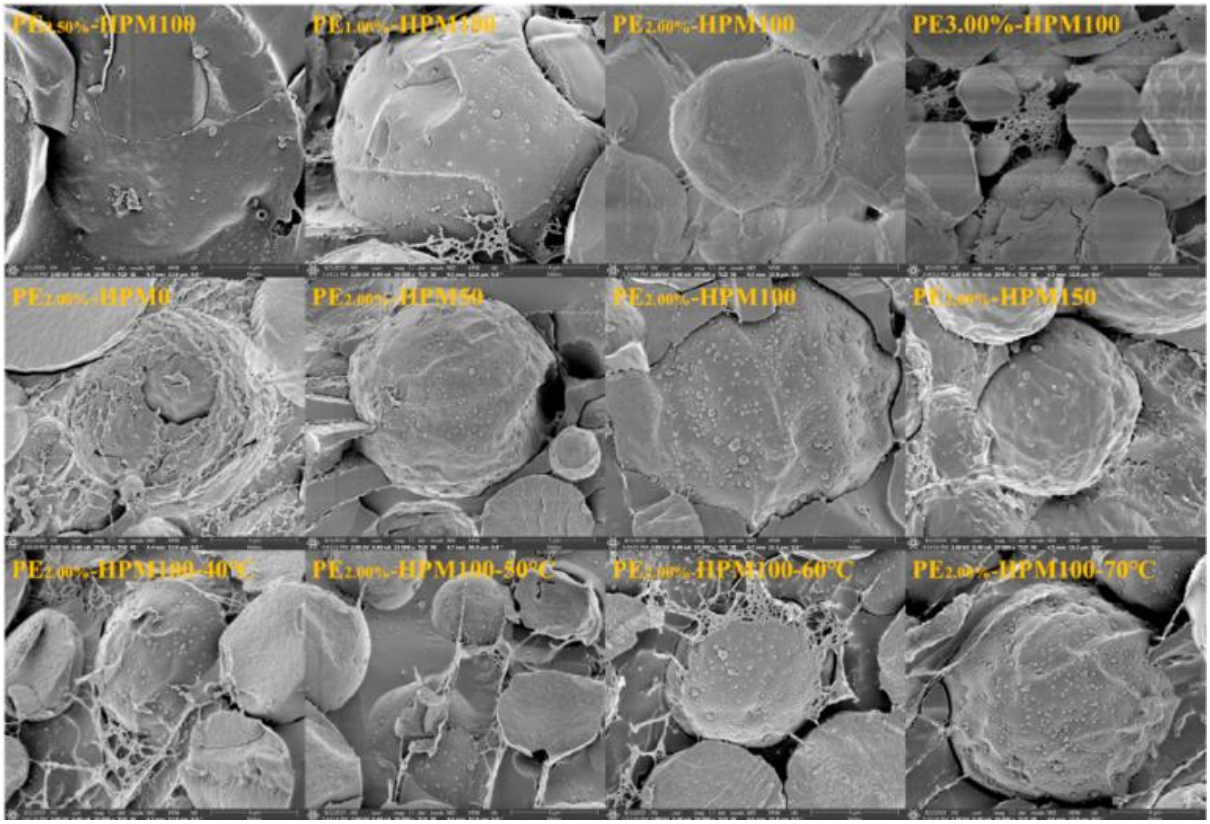

Fig. 6.Cryo-SEM microstructure of Pickering emulsions.

3.6. *In vitro* gastrointestinal digestion behaviour of Pickering emulsions

3.6.1. Droplet size

During gastrointestinal digestion, it was noted that the particle concentration showed a profound influence on the droplet size at each GIT phase (Fig. 7A). The largest increase in the droplet size occurred in $PE_{0.50\%}$-HPM100 and the emulsion stability was enhanced continuously with increasing the particle concentration. Within the gastric phase, the droplet aggregation occurred in all emulsions as a result of reduced electrostatic repulsion provided by nanoparticles at pH 2.0. At the lower particle concentration, the particles at the interface were insufficient to provide steric repulsion to retard the droplet aggregation (Fig. 7B). Besides, in an acidic environment, the nanoparticles with a low zeta-potential value were insufficient to provide the effective electrostatic repulsion. As the particle concentration increased, the rise in the droplet size was reduced. The particle-laden interface provided the sufficient protection for droplets in the stomach phase. This phenomenon also interpreted that complex nanoparticles remained relatively stable against gastric acid and pepsin as an interfacial stabilizer. It was reported that zein-based nanoparticles could resist the proteolysis in the gastric phase (Paliwal & Palakurthi, 2014). Within the small intestinal phase, the disaggregation of droplets might occur in $PE_{0.50\%}$-HPM100 due to the neutral pH. The rise in pH made the particles carry a large amount of negative charge again (data not shown), and the strong electrostatic repulsion segregated the aggregated droplets (Fig. 7C). In regards of the Pickering emulsions stabilized by the higher concentrations of nanoparticles, the droplet size was increased except for $PE_{2.00\%}$-HPM100, which was attributed to the digestion of lipid droplets due to the action of pancreatin and lipase (Lu et al., 2016).

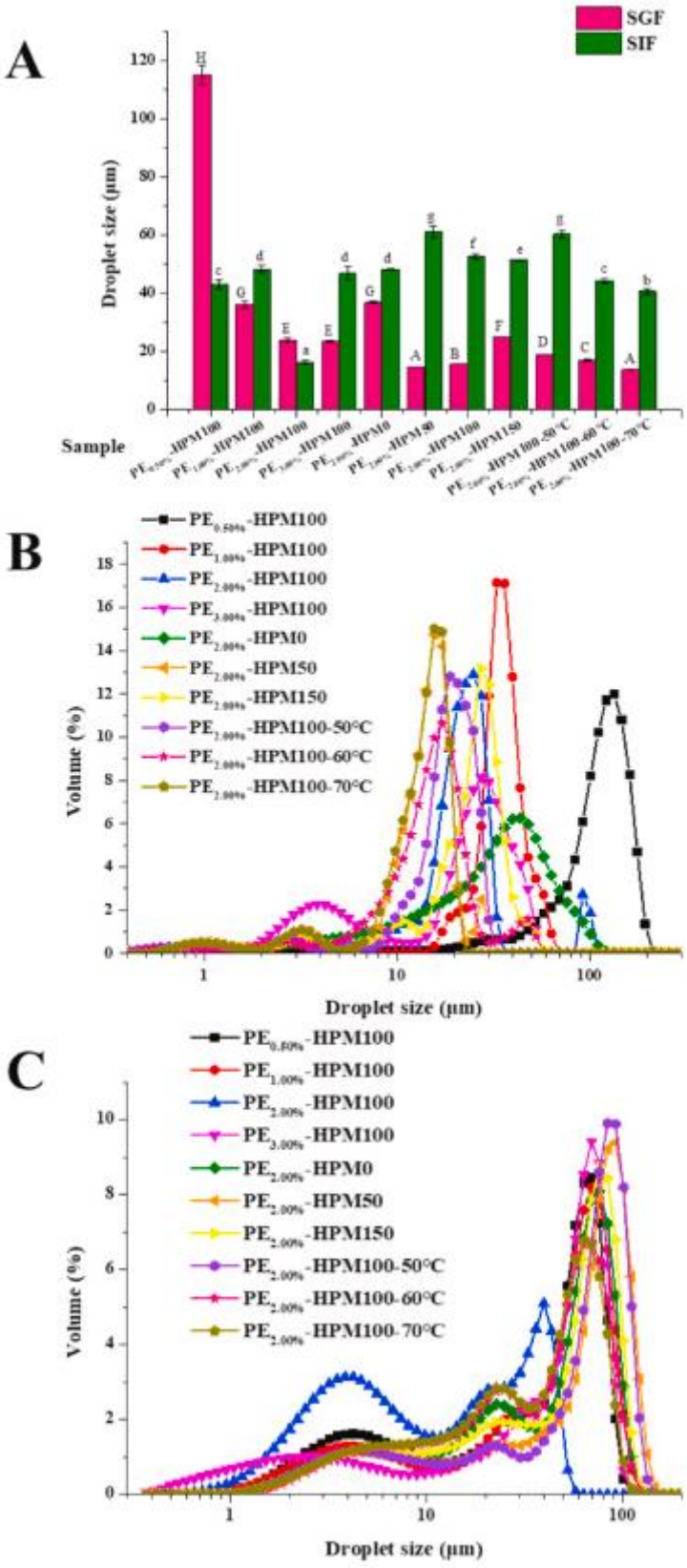

Fig. 7. Droplet size of Pickering emulsions during in vitro digestion (A); droplet size distribution of Pickering emulsions in gastric phase (B) and intestinal phase (C) (Different superscript letters (A, B, C ...) in the figure indicate significant differences (p <0.05) in droplet size in SGF; different superscript letters (a, b, c ...) in the figure indicate significant differences (p <0.05) in droplet size in SIF).

In terms of Pickering emulsions treated by different pressures, the largest increase was observed in the droplet size of $PE_{2.00\%}$-HPM0 (Fig. 7A). As aforementioned, the lipid droplets that have not passed through the microfluidization were likely to form particle bridging with the subsequent droplet aggregation. Under the acidic condition of gastric phase, the negative charge of nanoparticles was decreased and therefore the electrostatic repulsion between droplets was reduced, resulting in further flocculation (Fig. 7B). The Pickering emulsions that treated through microfluidization showed a better stability in the gastric phase. Interestingly, within the small intestinal phase, the magnitude of increase in the droplet size treated by microfluidization was greater than that of ones in the absence of microfluidization. The lipid droplets of emulsions that have not undergone microfluidization became more flocculated, which limited their active surface, thereby reducing the adsorption of bile salts and lipases onto the droplet surface and inhibited the lipolysis (Fig. 7C) (Bai et al., 2019b). Nevertheless, the Pickering emulsions with microfluidization showed an uniform state. The droplets were evenly distributed and the space between the droplets was larger with the exposure of more available surface, thereby promoting the lipolysis in the small intestine (Lin, Liang, Ye, Singh, & Zhong, 2017). During the gastric digestion, there was no significant difference observed in the Pickering emulsions pre-heated at different temperatures, and they still maintained a good stability in the presence of gastric acids and pepsin (Fig. 7A and B). As the heating temperature increased, the droplet size of Pickering emulsions increased more slowly in the intestinal phase, which showed the improved resistance against environmental changes during the intestinal digestion (Fig. 7C). These results might be because heating increased the droplet size and reduced the accessible surface area, subsequently inhibiting the adsorption of bile salts and digestive enzymes (Sarkar, Zhang, Holmes, & Ettelaie, 2019, January 1).

3.6.2. Microstructure

The microstructure of Pickering emulsions during gastrointestinal digestion was observed through CLSM. As shown in Fig. 8, the droplet coalescence occurred in all emulsions when transferred from gastric to intestinal phase, except for $PE_{0.50\%}$-HPM0. With the aid of CLSM, many irregular lipid droplets and smaller ones could be observed, which reflected the multimodal distribution of droplet sizes. This phenomenon was due to the addition of bile salts and pancreatin, which facilitated the hydrolysis of triglycerides. Furthermore, the adsorption of bile salts and lipase might promote the nanoparticles to desorb from the interface, resulting in the destabilization of Pickering emulsions in the small intestine. Alternatively, bile salts and lipases may bind directly to particle surfaces and alter the properties of adsorbed particles.

3.6.3. Lipid digestion

The influence of particle concentration, microfluidization pressure and heating temperature on the FFA release from Pickering emulsions was investigated. When the particle concentration was 0.50 % (w/v), the Pickering emulsion showed the lowest initial release rate and extent of FFA during the intestinal digestion (Fig. 9A). The droplet flocculation reduced the accessible surface area, retarding the adsorption of bile salts and lipases on the interface, and thus inhibiting the hydrolysis of tri-glycerides. Noticeably, after the initial 10 min of digestion in the small intestine, the release rate of FFA increased rapidly. The enhanced electrostatic repulsion between droplets and the emulsifying effect of bile salts in the neutral environment could help to enlarge the surface area and promote the adsorption of lipase on the droplet surface, thereby accelerating the lipolysis. As the particle concentration increased, the initial release rate and total release amount of FFA gradually decreased. As the particle concentration was 0.50 %, 1.00 %, 2.00 %, and 3.00 % (w/v), the total release amounts of FFA in Pickering emulsions after intestinal digestion were 16.11 %, 15.54 %, 13.42 % and 9.09 %, respectively. This phenomenon interpreted that the elevated interfacial particle concentration could

effectively delay the hydrolysis of tri-glycerides and the release of FFA. The particles attached at the interface were difficult to be displaced by bile salts because of energy barrier, and the negatively charged nanoparticles generated electrostatic repulsion against the adsorption of negatively charged bile salts. Therefore, bile salts could only occupy the interfacial gaps between nanoparticles, promoting the adsorption of lipase/co-lipase. Nevertheless, the enhanced adsorption of particles on the droplet surface decreased the gap between the nanoparticles, thereby reducing the accessible area of bile salts and lipase to the droplet surface, and inhibiting the lipolysis (Sarkar et al., 2019; Wei, Tong, Dai, Wang, Lv, Liu, Mao, & Yuan, 2020).

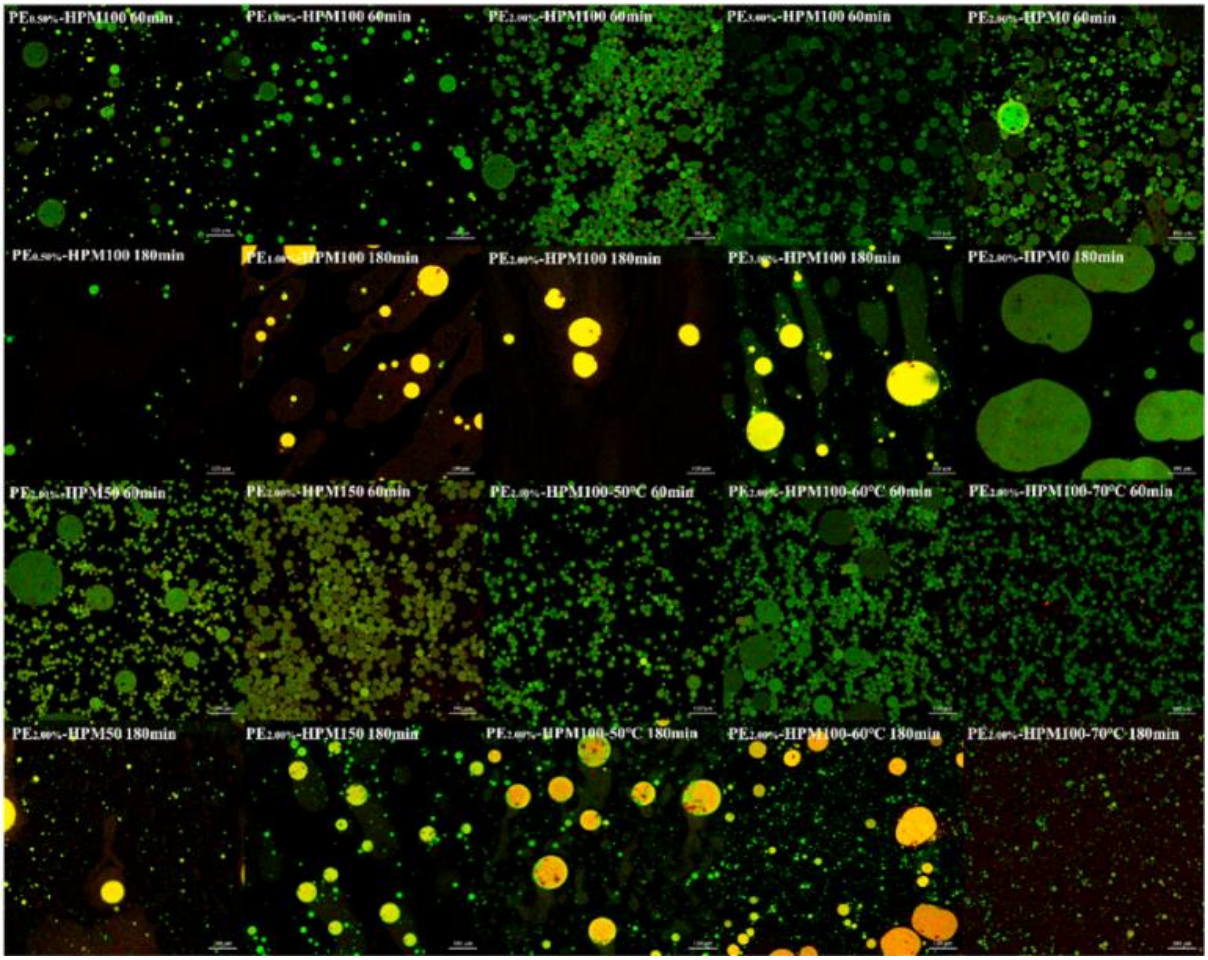

Fig. 8.Effects of particle concentration, microfluidization pressure and heating temperature on the microstructure of Pickering emulsions after digestion in gastric phase and intestinal phase.

After being mircofluidized, there was no significant effect on the release rate of FFA in Pickering emulsions at 50 MPa (Fig. 9B). When the pressure was elevated to 100 MPa, the initial release rate and total release amount of FFA increased and reached the maximum. This phenomenon might be due to the fact that the microfluidization reduced the droplet size and generated the larger space between droplets. The enlarged surface area of droplets facilitated the adsorption of bile salts and then lipases, thereby promoting the hydrolysis of triglycerides. Nevertheless, when the applied pressure continued to increase to 150 MPa, the amount of FFA release reversely decreased. The higher pressure might over-process Pickering emulsions, causing the partial aggregation and even a slight increase in the droplet size, reducing the surface area of droplets, thereby inhibiting the lipolysis (Bai et al., 2019a).

The pre-heated Pickering emulsions exhibited an obvious decrease in FFA release, although different heating temperatures showed a small distinction (Fig. 9C). Compared with the control group without thermal treatment, the release rates of FFA in the emulsions pre-heated at 50, 60 and 70 ◦C were decreased to 5.51 %, 6.07 % and 5.65 %, respectively. This might be attributed to that thermal treatment promoting the droplets to aggregate rather than coalescence, and reducing the surface area of droplets accessible to bile salts and lipase in the intestinal plase, thereby inhibiting lipolysis of Pickering emulsions. Additionally, thermal treatment might cause the fusion and bridging of particles at the interface, further promoting the wrapping and covering of lipid droplets, which then limited the permeation of bile salts and lipases into the interfacial layer and reduced the formation of FFA.

3.6.4. Bioaccessibility of curcumin and β-carotene

The release of nutraceuticals from food matrices in gastrointestinal fluids is the premise of determining their bioaccessibility. The endogenous factor affecting the bioaccessibility of bioactives is the solubilization capacity of mixed micelles formed in the small intestine, dependent on the digestible lipids consumed and the molecular characteristics of bioactives (Dima, Assadpour, Dima, & Jafari, 2020; Sarkar & Mackie, 2020). In present study, the bioaccessibility of curcumin (nanoparticles) was much higher than β-carotene (lipid droplet) in most emulsions (Fig. 9D). Recent studies have shown that medium chain triglyceride (MCT) in this study formed mixed micelles with smaller dimensions compared to long chain triglyceride (LCT), which restricted the fraction of bioactives could be incorporated into micellar phase. Meanwhile, β-carotene usually exhibited a lower bioaccessibility than curcumin due to the considerably larger molecular sizes (Yao, Xiao, & McClements, 2014). The small size of nanoparticles led to a higher release rate of curcumin with the increase in the surface area accessible to lipolytic enzymes. As reported before, the small size of nanoparticles favored the adsorption through the layer of epithelial cells (Dima et al., 2020). In this study, curcumin and β-carotene were solubilized by inclusion in the mixed micelles composed of bile salts, polypeptides (derived from the enzymolysis from proteins), TS and FFAs released.

The bioaccessibility of curcumin was dependent on the concentration of nanoparticles at the interface. As the particle concentration was increased from 0.50 % to 3.00 % (w/v), the curcumin bioaccessibility was decreased gradually from 75.33 ±5.11 % to 35.93 ±0.52 % (Fig. 9D). This was because the increased amount of particles at the interface reduced the active surface area, retarding the contact of bile salts and lipase to droplets, thus inhibiting the hydrolysis of fat and the release of FFA, influencing the formation of mixed micelles (Sarkar et al., 2019). Furthermore, the higher particle concentration increased the content of curcumin embedded. Upon fixing the content of oil and β-carotene entrapped in the Pickering emulsions, the limited micelle content determined its ability to dissolve lipophilic nutrients, which reduced the bioaccessibility of curcumin when more curcumin was added (Wei, Yu, et al., 2019). The highest β-carotene bioaccessibility was obtained in $PE_{1.00\%}$-HPM100. When the particle concentration was increased from 1.0 % to 3.0 % (w/v), the β-carotene bioaccessibility was decreased from 19.46 ±0.59 % to 13.13 ±1.37 %, which was much lower than the curcumin bioaccessibility. On one hand, as aforementioned, more interfacial particles limited the release of FFA during the digestion, which reduced the formation of mixed micelles for solubilization of β-carotene. On the other hand, the limited volume of hydrophobic region inside the mixed micelle restricted its ability to dissolve and contain lipophilic molecules (Guo, Ye, Bellissimo, Singh, & Rousseau, 2017). Compared to curcumin, β-carotene has a higher molecular weight, which restricted its incorporation into mixed micelles (Yao et al., 2014).

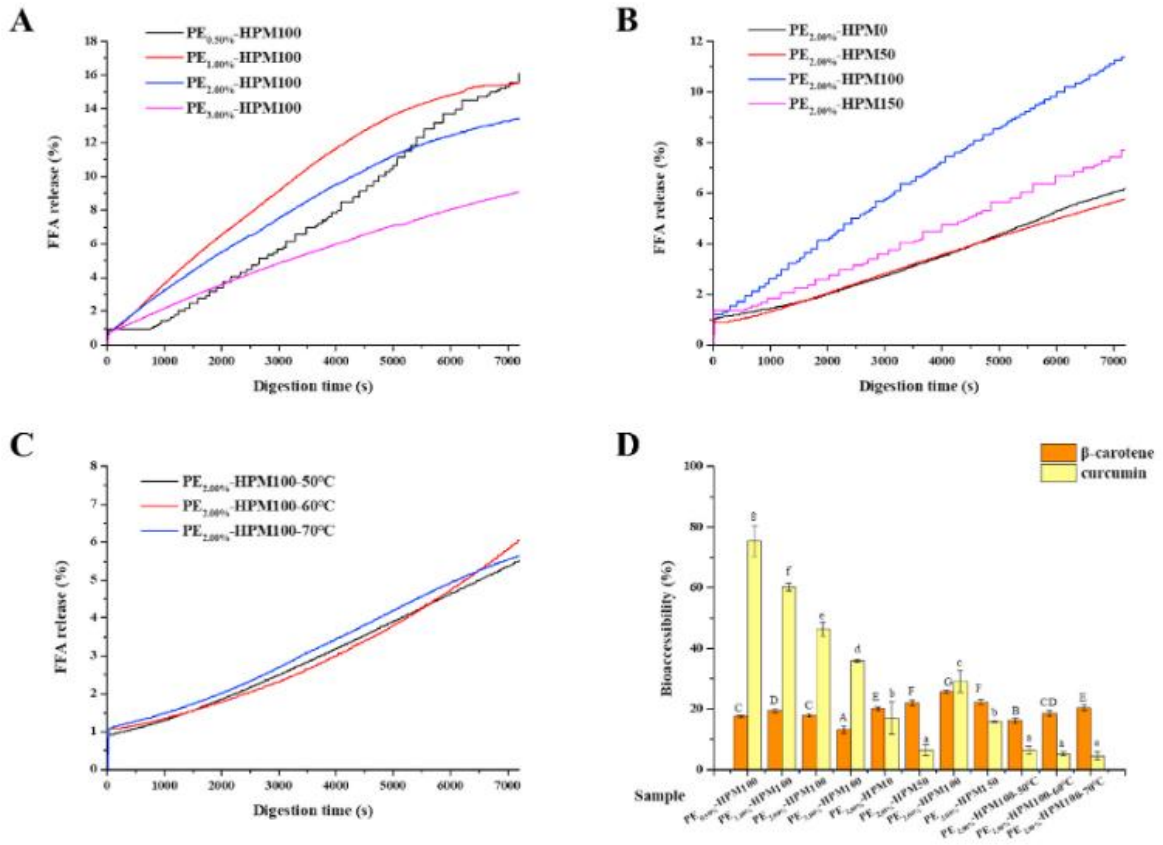

Fig. 9. Influence of microfluidization pressure (A), particle concentration (B) and heating temperature (C) on the release rate of total available free fatty acids (FFAs) as a function of time during intestinal digestion; bioaccessibility of β-carotene and curcumin (D) (Different superscript letters (A, B, C ...) in the figure indicate significant differences (p <0.05) in the bioaccessibility of β-carotene; different superscript letters (a, b, c ...) in the figure indicate significant differences (p <0.05) in the bioaccessibility of curcumin).

After microfluidization, the bioaccessibility of nutraceuticals was consistent with the FFA release rate of Pickering emulsions: the bioaccessibility of curcumin and β-carotene was firstly increased with the rise in the pressure, and reached the maximum at 100 MPa; but when the homogenizing pressure rose to 150 MPa, the bioaccessibility of nutraceuticals was decreased (Fig. 9D). This phenomenon was because different pressures influenced the structure and droplet size of Pickering emulsions. When the pressure was elevated from 0 to 100 MPa, the emulsion became more uniform with the smaller droplet size, which increased the surface area of droplets and then the adsorption of bile salts, thereby promoting the hydrolysis of grease and the formation of mixed micelles (Li & Julian McClements, 2010). Nevertheless, as the microfluidization pressure was elevated at a higher level, the part of droplets aggregated with the increased droplet size, thereby reducing the surface area, which decreased the FFA release rate and bioaccessibility of nutraceuticals. When Pickering emulsions were pre-heated and then subjected to microfluidization, the bioaccessibility of nutraceuticals has decreased and was related to the heating temperature. As the Pickering emulsion was pre-heated at 50 ◦C, the bioaccessibility of β-carotene was decreased to 16.24 ±0.82 %. The thermal treatment caused the droplet flocculation, which reduced the accessible surface area, thus subsequently inhibiting the contact with bile salts and lipases in the intestinal phase. Thereafter, the decreased FFA release rate retarded the formation of mixed micelles in the small intestine, thereby reducing the β-carotene bioaccessibility. With increasing the heating temperature, the bioaccessibility of β-carotene in Pickering emulsions rose to 18.55 ±0.94 % at 60 ◦C and 20.38 ±0.84 % at 70 ◦C. This phenomenon might be due to the thermal treatment at the higher temperature that induced the particle

aggregation at the interface, which increased the surface area exposed. Meanwhile, the bioaccessibility of curcumin decreased greatly through thermal treatment, even lower than that of β-carotene, revealing that the influence of thermal treatment on the interfacial nanoparticles might be greater than droplets. The particle aggregation induced by thermal treatment affected the digestive behaviour of complex nanoparticles, thereby inhibiting the release of curcumin in the small intestinal phase.

4. Conclusion

In this study, both the microfluidization pressure and particle concentration exhibited significant impacts on the physicochemical stability, microstructure, and in vitro digestion of Pickering emulsions for the co-delivery of curcumin and β-carotene. The closely packed particle layer strengthened the steric and electrostatic repulsion among the droplets, which prevented the emulsion coalescence and protected both nutraceuticals. The encapsulation of curcumin into complex nanoparticles effectively enhanced the photothermal stability of β-carotene entrapped in emulsion droplets. The interfacial structure and stability of Pickering emulsions influenced their digestion fate within the GIT. Through modulating the particle concentration, heating temperature and homogenization pressure, the digestive fate of Pickering emulsion and bioaccessibility of bioactives could be regulated. The higher particle concentration and heating temperature retarded the FFA release from lipid droplets with lower bioaccessibility of curcumin and β-carotene. Conversely, the microfluidization at the lower pressure (≤100 MPa) promoted the lipolysis and increased the bioaccessibility of nutraceuticals in Pickering emulsions in the small intestine. These findings showed a promising strategy of designing the Pickering emulsion coloaded with multiple nutrients via combined microfluidization and heating treatment, providing a new insight into optimizing their functional properties by regulating processing conditions.

Notes

The authors declare no competing financial interest.

Author statement

Yang Wei: Conceptualization, Methodology, Writing- Original draft preparation. Chao Wang: Data curation, Validation, Methodology. Xin Liu: Software. Alan Mackie: Revision. Mengke Zhang: Methodology. Lei Dai: Investigation. Jinfang Liu: Supervision. Like Mao: Software. Fang Yuan: Validation. Yanxiang Gao: Writing- Reviewing and Editing.

Declaration of competing interest

The authors declare no competing financial interest in this study. Acknowledgement The research was funded by the National Natural Science Foundation of China (No. 31871842). The authors are grateful to Tsinghua University Branch of China National Center Protein Sciences (Beijing, China) for providing the facility support of Cryo-SEM with the aid of Xiaomin Li.

References

Araiza-Calahorra, A., Akhtar, M., & Sarkar, A. (2018). Recent advances in emulsion- based delivery approaches for curcumin: From encapsulation to bioaccessibility. Trends in Food Science & Technology, 71(September 2017), 155–169. https://doi.org/ 10.1016/j.tifs.2017.11.009

Bai, L., Lv, S., Xiang, W., Huan, S., McClements, D. J., & Rojas, O. J. (2019a). Oil-in-water pickering emulsions via microfluidization with cellulose nanocrystals: 1. Formation and stability. Food Hydrocolloids, 96(April), 699–708. https://doi.org/10.1016/j. foodhyd.2019.04.038

Bai, L., Lv, S., Xiang, W., Huan, S., McClements, D. J., & Rojas, O. J. (2019b). Oil-in-water pickering emulsions via microfluidization with cellulose nanocrystals: 1. Formation and stability. Food Hydrocolloids, 96(January), 699–708. https://doi.org/10.1016/j. foodhyd.2019.04.038
Bai, L., Lv, S., Xiang, W., Huan, S., McClements, D. J., & Rojas, O. J. (2019c). Oil-in-water pickering emulsions via microfluidization with cellulose nanocrystals: 2. In vitro lipid digestion. Food Hydrocolloids, 96(April), 709–716. https://doi.org/10.1016/j. foodhyd.2019.04.039
Bai, L., & McClements, D. J. (2016). Formation and stabilization of nanoemulsions using biosurfactants: Rhamnolipids. Journal of Colloid and Interface Science, 479, 71–79. https://doi.org/10.1016/J.JCIS.2016.06.047
Binks, B. P. (2002). Particles as surfactants—similarities and differences. Current Opinion in Colloid & Interface Science, 7(1–2), 21–41. https://doi.org/10.1016/S1359-0294 (02)00008-0
Binks, B. P., Desforges, A., & Duff, D. G. (2007). Synergistic stabilization of emulsions by a mixture of surface-active nanoparticles and surfactant. Langmuir, 23(3), 1098–1106. https://doi.org/10.1021/la062510y
Bordoloi, D., & Kunnumakkara, A. B. (2018). The potential of curcumin: A multitargeting agent in cancer cell chemosensitization. Role of Nutraceuticals in Cancer Chemosensitization, 31–60. https://doi.org/10.1016/B978-0-12-812373-7.00002-4
Chen, G., Wang, S., Feng, B., Jiang, B., & Miao, M. (2019). Interaction between soybean protein and tea polyphenols under high pressure. Food Chemistry, 277(November 2018), 632–638. https://doi.org/10.1016/j.foodchem.2018.11.024
Dai, L., Sun, C., Wei, Y., Mao, L., & Gao, Y. (2018). Characterization of Pickering emulsion gels stabilized by zein/gum Arabic complex colloidal nanoparticles. Food Hydrocolloids, 74, 239–248. https://doi.org/10.1016/J.FOODHYD.2017.07.040
Dickinson, E. (2015). Structuring of colloidal particles at interfaces and the relationship to food emulsion and foam stability. Journal of Colloid and Interface Science, 449, 38–45. https://doi.org/10.1016/j.jcis.2014.09.080
Dickinson, E. (2017). Biopolymer-based particles as stabilizing agents for emulsions and foams. Food Hydrocolloids, 68, 219–231. https://doi.org/10.1016/J. FOODHYD.2016.06.024
Dima, C., Assadpour, E., Dima, S., & Jafari, S. M. (2020). Bioavailability of nutraceuticals: Role of the food matrix, processing conditions, the gastrointestinal tract, and nanodelivery systems. Comprehensive Reviews in Food Science and Food Safety, 1–41. https://doi.org/10.1111/1541-4337.12547 (January).
Donhowe, E. G., & Kong, F. (2014, February 1). Beta-carotene: Digestion, microencapsulation, and in vitro bioavailability. Food and Bioprocess Technology, 7, 338–354. https://doi.org/10.1007/s11947-013-1244-z
Fan, Y., Liu, Y., Gao, L., Zhang, Y., & Yi, J. (2018). Improved chemical stability and cellular antioxidant activity of resveratrol in zein nanoparticle with bovine serum albumin-caffeic acid conjugate. Food Chemistry, 261, 283–291. https://doi.org/ 10.1016/J.FOODCHEM.2018.04.055
French, D. J., Taylor, P., Fowler, J., & Clegg, P. S. (2015). Making and breaking bridges in a Pickering emulsion. Journal of Colloid and Interface Science, 441, 30–38. https:// doi.org/10.1016/J.JCIS.2014.11.032
Guo, Q., Ye, A., Bellissimo, N., Singh, H., & Rousseau, D. (2017). Modulating fat digestion through food structure design. Progress in Lipid Research, 68(August), 109–118. https://doi.org/10.1016/j.plipres.2017.10.001
Håkansson, A., Fuchs, L., Innings, F., Revstedt, J., Tragårdh, C., & Bergenståhl, B. (2011). High resolution experimental measurement of turbulent flow field in a high pressure homogenizer model and its implications on turbulent drop fragmentation. Chemical Engineering Science, 66(8), 1790–1801. https://doi.org/10.1016/J.CES.2011.01.026

Håkansson, A., & Rayner, M. (2018). General principles of nanoemulsion formation by high-energy mechanical methods. Nanoemulsions, 103–139. https://doi.org/ 10.1016/B978-0-12-811838-2.00005-9
Li, Y., & Julian McClements, D. (2010). New mathematical model for interpreting pH-stat digestion profiles: Impact of lipid droplet characteristics on in vitro digestibility. Journal of Agricultural and Food Chemistry, 58(13), 8085–8092. https://doi.org/ 10.1021/jf101325m
Lin, Q., Liang, R., Ye, A., Singh, H., & Zhong, F. (2017). Effects of calcium on lipid digestion in nanoemulsions stabilized by modified starch: Implications for bioaccessibility of β-carotene. Food Hydrocolloids, 73, 184–193. https://doi.org/ 10.1016/J.FOODHYD.2017.06.024
Liu, F., Ma, C., Zhang, R., Gao, Y., & Julian McClements, D. (2017). Controlling the potential gastrointestinal fate of β-carotene emulsions using interfacial engineering: Impact of coating lipid droplets with polyphenol-protein-carbohydrate conjugate. Food Chemistry, 221, 395–403. https://doi.org/10.1016/j.foodchem.2016.10.057
Liu, F., & Tang, C. H. (2016). Reprint of "Soy glycinin as food-grade Pickering stabilizers: Part. III. Fabrication of gel-like emulsions and their potential as sustained-release delivery systems for β-carotene. Food Hydrocolloids, 60(January), 631–640. https:// doi.org/10.1016/j.foodhyd.2016.05.004
Liu, F., Wang, D., Xu, H., Sun, C., & Gao, Y. (2016). Physicochemical properties of β-carotene emulsions stabilized by chlorogenic acid–lactoferrin–glucose/ polydextrose conjugates. Food Chemistry, 196, 338–346. https://doi.org/10.1016/J. FOODCHEM.2015.09.047
Lu, W., Kelly, A. L., Maguire, P., Zhang, H., Stanton, C., & Miao, S. (2016). Correlation of emulsion structure with cellular uptake behavior of encapsulated bioactive nutrients: Influence of droplet size and interfacial structure. Journal of Agricultural and Food Chemistry, 64(45), 8659–8666. https://doi.org/10.1021/acs.jafc.6b04136
Mao, L., Wang, D., Liu, F., & Gao, Y. (2018, March 24). Emulsion design for the delivery of β-carotene in complex food systems. Critical Reviews in Food Science and Nutrition, 58, 770–784. https://doi.org/10.1080/10408398.2016.1223599
Mao, L., Yang, J., Xu, D., Yuan, F., & Gao, Y. (2010). Effects of homogenization models and emulsifiers on the physicochemical properties of β-carotene nanoemulsions. Journal of Dispersion Science and Technology, 31(7), 986–993. https://doi.org/ 10.1080/01932690903224482
McClements, D. J., & Gumus, C. E. (2016). Natural emulsifiers — biosurfactants, phospholipids, biopolymers, and colloidal particles: Molecular and physicochemical basis of functional performance. Advances in Colloid and Interface Science, 234, 3–26. https://doi.org/10.1016/j.cis.2016.03.002
Minekus, M., Alminger, M., Alvito, P., Ballance, S., Bohn, T., Bourlieu, C., et al. (2014). A standardised static in vitro digestion method suitable for food-an international consensus. Food and Function, 5(6), 1113–1124. https://doi.org/10.1039/ c3fo60702j
Mulet-Cabero, A.-I., Egger, L., Portmann, R., Ḿenard, O., Marze, S., Minekus, M., et al. (2020). A standardised semi-dynamic in vitro digestion method suitable for food – an international consensus. Food & Function. https://doi.org/10.1039/c9fo01293a
Paliwal, R., & Palakurthi, S. (2014). Zein in controlled drug delivery and tissue engineering. Journal of Controlled Release, 189, 108–122. https://doi.org/10.1016/J. JCONREL.2014.06.036
Patel, A. R., & Velikov, K. P. (2014). Zein as a source of functional colloidal nano- and microstructures. Current Opinion in Colloid & Interface Science, 19(5), 450–458. https://doi.org/10.1016/j.cocis.2014.08.001
Pawar, A. B., Caggioni, M., Ergun, R., Hartel, R. W., & Spicer, P. T. (2011). Arrested coalescence in Pickering emulsions. Soft Matter, 7(17), 7710–7716. https://doi.org/ 10.1039/c1sm05457k
Perrier-Cornet, J. M., Marie, P., & Gervais, P. (2005). Comparison of emulsification efficiency of protein-stabilized oil-in-water emulsions using jet, high pressure and colloid mill homogenization. Journal of Food Engineering, 66(2), 211–217. https:// doi.org/10.1016/J.JFOODENG.2004.03.008

Sanidad, K. Z., Sukamtoh, E., Xiao, H., McClements, D. J., & Zhang, G. (2019). Curcumin: Recent advances in the development of strategies to improve oral bioavailability. Annual Review of Food Science and Technology, 10(1), 597–617. https://doi.org/ 10.1146/annurev-food-032818-121738
Sarkar, A., & Mackie, A. R. (2020). Engineering oral delivery of hydrophobic bioactives in real-world scenarios. Current Opinion in Colloid & Interface Science, 48, 40–52. https://doi.org/10.1016/j.cocis.2020.03.009
Sarkar, A., Zhang, S., Holmes, M., & Ettelaie, R. (2019, January 1). Colloidal aspects of digestion of Pickering emulsions: Experiments and theoretical models of lipid digestion kinetics. Advances in Colloid and Interface Science, 263, 195–211. https:// doi.org/10.1016/j.cis.2018.10.002
Sriamornsak, P., Thirawong, N., Cheewatanakornkool, K., Burapapadh, K., & Sae- Ngow, W. (2008). Cryo-scanning electron microscopy (cryo-SEM) as a tool for studying the ultrastructure during bead formation by ionotropic gelation of calcium pectinate. International Journal of Pharmaceutics, 352(1–2), 115–122. https://doi. org/10.1016/J.IJPHARM.2007.10.038
Tikekar, R. V., Pan, Y., & Nitin, N. (2013). Fate of curcumin encapsulated in silica nanoparticle stabilized Pickering emulsion during storage and simulated digestion. Food Research International, 51(1), 370–377. https://doi.org/10.1016/j. foodres.2012.12.027
Wang, Y., & Padua, G. W. (2010). Formation of zein microphases in ethanol-water. Langmuir, 26(15), 12897–12901. https://doi.org/10.1021/la101688v Weber, D., & Grune, T. (2012). The contribution of β-carotene to vitamin A supply of humans. Molecular Nutrition & Food Research, 56(2), 251–258. https://doi.org/ 10.1002/mnfr.201100230
Wei, Y., Li, C., Zhang, L., Dai, L., Yang, S., Liu, J., et al. (2020). Influence of calcium ions on the stability, microstructure and in vitro digestion fate of zein-propylene glycol alginate-tea saponin ternary complex particles for the delivery of resveratrol. Food Hydrocolloids, 106(17), Article 105886. https://doi.org/10.1016/j. foodhyd.2020.105886
Wei, Y., Sun, C., Dai, L., Mao, L., Yuan, F., & Gao, Y. (2019a). Novel bilayer emulsions costabilized by zein colloidal particles and propylene glycol alginate, Part 1: Fabrication and characterization [Research-article]. Journal of Agricultural and Food Chemistry, 67(4), 1197–1208. https://doi.org/10.1021/acs.jafc.8b03240
Wei, Y., Sun, C., Dai, L., Mao, L., Yuan, F., & Gao, Y. (2019b). Novel bilayer emulsions costabilized by zein colloidal particles and propylene glycol alginate, Part 1: Fabrication and characterization. Journal of Agricultural and Food Chemistry, 67(4), 1197–1208. https://doi.org/10.1021/acs.jafc.8b03240
Wei, Y., Sun, C., Dai, L., Zhan, X., & Gao, Y. (2018). Structure, physicochemical stability and in vitro simulated gastrointestinal digestion properties of β-carotene loaded zein-propylene glycol alginate composite nanoparticles fabricated by emulsification- evaporation method. Food Hydrocolloids, 81, 149–158. https://doi.org/10.1016/j. foodhyd.2018.02.042
Wei, Y., Tong, Z., Dai, L., Ma, P., Zhang, M., Liu, J., et al. (2020a). Novel colloidal particles and natural small molecular surfactants co-stabilized Pickering emulsions with hierarchical interfacial structure: Enhanced stability and controllable lipolysis. Journal of Colloid and Interface Science, 563, 291–307. https://doi.org/10.1016/J. JCIS.2019.12.085
Wei, Y., Tong, Z., Dai, L., Wang, D., Lv, P., Liu, J., et al. (2020b). Author contributions Statement: Yang Wei: Conceptualization, methodology, software, writing- original. Food Hydrocolloids. , Article 105738. https://doi.org/10.1016/j. foodhyd.2020.105738
Wei, Y., Wang, C., Liu, X., Liao, W., Zhang, L., Chen, S., et al. (2021). Effects of microfluidization and thermal treatment on characterization and digestion of curcumin loaded protein-polysaccharide-tea saponin complex nanoparticles. Food & Function. https://doi.org/10.1039/d0fo02283g
Wei, Y., Yu, Z., Lin, K., Sun, C., Dai, L., Yang, S., et al. (2019). Fabrication and characterization of resveratrol loaded zein-propylene glycol alginate-rhamnolipid composite nanoparticles:

Physicochemical stability, formation mechanism and in vitro digestion. Food Hydrocolloids, 95, 336–348. https://doi.org/10.1016/j. foodhyd.2019.04.048
Winuprasith, T., Khomein, P., Mitbumrung, W., Suphantharika, M., Nitithamyong, A., & McClements, D. J. (2018). Encapsulation of vitamin D3 in pickering emulsions stabilized by nanofibrillated mangosteen cellulose: Impact on in vitro digestion and bioaccessibility. Food Hydrocolloids, 83(May), 153–164. https://doi.org/10.1016/j. foodhyd.2018.04.047
Xiao, Y., Chen, C., Wang, B., Mao, Z., Xu, H., Zhong, Y., et al. (2018). Vitro digestion of oil-in-water emulsions stabilized by regenerated chitin. Journal of Agricultural and Food Chemistry, 66(46), 12344–12352. https://doi.org/10.1021/acs.jafc.8b03873
Xiao, J., Li, Y., & Huang, Q. (2016). Recent advances on food-grade particles stabilized Pickering emulsions: Fabrication, characterization and research trends. Trends in Food Science & Technology, 55, 48–60. https://doi.org/10.1016/J.TIFS.2016.05.010
Xiao, J., Nian, S., & Huang, Q. (2015). Assembly of kafirin/carboxymethyl chitosan nanoparticles to enhance the cellular uptake of curcumin. Food Hydrocolloids, 51, 166–175. https://doi.org/10.1016/J.FOODHYD.2015.05.012
Yao, M., Xiao, H., & McClements, D. J. (2014). Delivery of lipophilic bioactives: Assembly, disassembly, and reassembly of lipid nanoparticles. Annual Review of Food Science and Technology, 5(1), 53–81. https://doi.org/10.1146/annurev-food-072913- 100350
Yi, J., Liu, Y., Zhang, Y., & Gao, L. (2018). Fabrication of resveratrol-loaded whey protein-dextran colloidal complex for the stabilization and delivery of β-carotene emulsions [Research-article]. Journal of Agricultural and Food Chemistry, 66(36), 9481–9489. https://doi.org/10.1021/acs.jafc.8b02973
Zhang, L., McClements, D. J., Wei, Z., Wang, G., Liu, X., & Liu, F. (2019). Delivery of synergistic polyphenol combinations using biopolymer-based systems: Advances in physicochemical properties, stability and bioavailability. Critical Reviews in Food Science and Nutrition, 1–15. https://doi.org/10.1080/10408398.2019.1630358
Zhu, Z., Wen, Y., Yi, J., Cao, Y., Liu, F., & McClements, D. J. (2019). Comparison of natural and synthetic surfactants at forming and stabilizing nanoemulsions: Tea saponin, Quillaja saponin, and Tween 80. Journal of Colloid and Interface Science, 536, 80–87. https://doi.org/10.1016/j.jcis.2018.10.024
Zou, Y., Guo, J., Yin, S.-W., Wang, J.-M., & Yang, X.-Q. (2015). Pickering emulsion gels prepared by hydrogen-bonded zein/tannic acid complex colloidal particles. Journal of Agricultural and Food Chemistry, 63(33), 7405–7414. https://doi.org/10.1021/acs. jafc.5b03113